doi:10.1006/jmbi.2000.4342 available online at http://www.idealibrary.com on IDEAL® *J. Mol. Biol.* (2001) **305**, 1111–1129

JMB

The scFv Fragment of the Antibody hu4D5-8: Evidence for Early Premature Domain Interaction in Refolding

Marcus Jäger, Peter Gehrig and Andreas Plückthun*

Biochemisches Institut
Universität Zürich
Winterthurerstr. 190
CH-8057 Zürich
Switzerland

**Corresponding author*

Fluorescence spectroscopy and $^1H/^2H$-exchange techniques have been applied to characterize the folding of an scFv fragment, derived from the humanized anti-HER2 antibody hu4D5-8. A stable intermediate, consisting of a native V_L domain and an unfolded V_H domain, is populated under equilibrium unfolding conditions. A partially structured intermediate, with $^1H/^2H$-exchange protection significantly less than that of the two isolated domains together, is detectable upon refolding the equilibrium-denatured scFv fragment. This means that the domains in the heterodimer do not fold independently. Rather, they associate prematurely before full $^1H/^2H$-exchange protection can be gained. The formation of the native heterodimer from the non-native intermediate is a slow, cooperative process, which is rate-limited by proline *cis/trans*-isomerization. Unproductive domain association is also detectable after short-term denaturation, i.e. with the proline residues in native conformation. Only a fraction of the short-term denatured protein folds into the native protein in a fast, proline-independent reaction, because of spontaneous proline *cis/trans*-reisomerization in the early non-native intermediate. The comparison with the previously studied antibody McPC603 has now allowed us to delineate similarities in the refolding pathway of scFv fragments.

Keywords: protein folding; multidomain proteins; scFv fragment; $^1H/^2H$-exchange; mass spectrometry

Introduction

Despite some advances in the understanding of the folding of small, monomeric proteins, little is known about the folding of oligomeric proteins (Jaenicke, 1987). A key question related to these proteins is to what extent the folding pathway and stability of a domain or subunit is influenced by the presence of an interacting domain or subunit. Because of their modular architecture, antibodies are well suited for answering these questions (Padlan, 1994). The building block of antibodies is a domain of ~100 amino acid residues in length, which folds into a characteristic folding topology. Biophysical studies on the folding and stability on antibodies can be performed on the isolated constituting domains (Goto & Hamaguchi, 1982; Tsunenaga *et al.*, 1987; Steipe *et al.*, 1994) as well as on assemblies of these domains in various structural contexts of increasing complexity, such as the Fv and scFv fragment (Freund *et al.*, 1996; Jäger & Plückthun, 1999a,b; Ramm *et al.*, 1999), the Fab fragment (Lilie *et al.*, 1995), or even as part of the intact antibody (Lilie, 1997).

In our laboratory, much of the work on folding and unfolding of antibody Fv and scFv fragments had been concentrated on the phosphorylcholine binding antibody McPC603 (Freund *et al.*, 1996, 1997, 1998; Jäger & Plückthun, 1997, 1999a,b). The Fv fragment is an unlinked heterodimer composed of the V_H and V_L domains, whose interaction is

Abbreviations used: CDR, complementarity-determining region; ESI-MS, electrospray ionization mass spectrometry; Fv, antibody Fv fragment consisting of the unlinked V_H and V_L domain; GdmCl, guanidinium hydrochloride; $^1H/^2H$-exchange, hydrogen-deuterium exchange; IMAC, immobilized metal ion affinity chromatography; IPTG, isopropyl-β-D-thiogalactopyranoside; PCR, polymerase chain reaction; PPIase, peptidyl-prolyl *cis/trans*-isomerase; scFv, single-chain Fv fragment of an antibody, consisting of the V_H and V_L domain, connected by a flexible peptide linker; V_H, variable domain of an antibody heavy chain; V_L, variable domain of an antibody light chain.

E -mail address of the corresponding author: plueckthun@biocfebs.unizh.ch

0022-2836/01/051111–19 $35.00/0

stabilized by a large hydrophobic interface (Satow *et al.*, 1986). The domains refold fast and independently into compact intermediates from a chemically denatured state (4 M GdmCl). The rate-limiting step for the formation of the Fv heterodimer is the slow proline *cis/trans*-isomerization at an interface proline residue (ProL95), located at the edge of CDR3 of the V_L domain. ProL95 is not absolutely conserved, but is found at this position in the great majority of antibody κ-type V_L domains. It becomes buried in the hydrophobic interface, and a *cis*-conformation is critical for maintaining the quaternary structure of the Fv fragment. If the two domains are covalently tethered into an scFv fragment (scFv) by a flexible peptide linker ($(G_4S)_3$ or $(G_4S)_5$) in the format V_H-linker-V_L, independent domain folding is no longer possible. Instead, the two domains associate prematurely, leading to fewer exchange-protected ^2H in the scFv fragment than in the two isolated domains together. The return from this folding trap is rate limiting for the acquisition of the full protection, but not rate limiting for the overall refolding reaction, as the slow proline *cis/trans*-isomerization at ProL95 proceeds at an even slower rate.

In order to test whether the observations made for the Fv and scFv fragment of the antibody McPC603 are representative for other antibody fragments as well, we report experiments on the folding and stability of the scFv fragment and the V_H and V_L domains of the antibody 4D5-8 (Carter *et al.*, 1992a,b; Kelley *et al.*, 1992), which binds the extracellular domain of human epidermal growth factor receptor-2 ($p185^{HER2\text{-}ECD}$). We have chosen the antibody 4D5-8 as a model system (Ramm *et al.*, 1999) for several reasons. First, the X-ray crystal structure of the 4D5-8 Fv fragment has been determined (Eigenbrot *et al.*, 1993). Second, F_{ab}, Fv and scFv fragments of the antibody 4D5-8 can be expressed at high yields in *Escherichia coli* in soluble and functional form (Carter *et al.*, 1992b; Wörn & Plückthun, 1998b). Third, the fragments of 4D5-8 are rather stable towards thermal inactivation (Knappik & Plückthun, 1995). Finally, the hu4D5 framework, being itself the product of a humanization study, has been used in CDR grafting studies (Carter *et al.*, 1992a). Therefore, insights gained on the folding and assembly of the antibody 4D5-8 might have impact on other antibodies as well. The results obtained for the antibody 4D5-8 were compared to the previous data obtained for the McPC603 system, to highlight possible generalizations in the folding and assembly behavior of this type of biotechnologically and biomedically important class of proteins.

Results

Spectral properties of the antibody 4D5

The scFv fragment investigated here is the humanized scFv fragment of the anti-$p185^{HER2}$ antibody hu4D5-8 (Carter *et al.*, 1992a,b; Kelley *et al.*, 1992), abbreviated as 4D5 in this study. The V_L domain shows a fluorescence increase at > 320 nm upon unfolding, the V_H domain a fluorescence increase at > 336 nm (Figure 1(a)). Similar spectral changes have also been observed in the unfolding of the V_H and V_L domain of the antibody McPC603 (Jäger & Plückthun, 1999a). The fluorescence change in the V_L domain reports the increase in distance upon unfolding between the conserved core TrpL36 and the disulfide bond, which quenches TrpL36-fluorescence in the native protein. Less straightforward is the interpretation of the spectral changes in the V_H domain, since in addition to the core TrpH36, the three CDR-Trp residues (TrpH47, TrpH95, TrpH103) also contribute to the observed fluorescence change. The fluorescence emission spectrum of the native scFv fragment is different from a computational addition of the emission spectra of the isolated constituting domains at a 1:1 stoichiometry (Figure 1(b)). As previously shown for the Fv and the scFv fragment of the antibody McPC603 (Jäger & Plückthun, 1999a), this spectral change must be due to the fact that the CDR-Trp residues become buried in a hydrophobic interface upon heterodimerization. Therefore, the large fluorescence increase between about 320 and 340 nm is a convenient monitor of interface formation.

Evidence for an equilibrium unfolding intermediate in the scFv fragment

The thermodynamic stability of the isolated domains was investigated by monitoring the change in fluorescence intensity at 350 nm (V_L domain) (Figure 2(a)) or 375 nm (V_H domain) (Figure 2(b)) upon unfolding. Both unfolding transitions fit well to a two-state reaction with a linear free energy model (N⇌U) (Santoro & Bolen, 1988). A least-squares fit gives the following thermodynamic parameters: $\Delta G_{N\text{-}U}$ (V_L) = 36.8 kJ mol^{-1}; m_G (V_L) = 13.2 kJ mol^{-1} M^{-1}; $\Delta G_{N\text{-}U}$ (V_H) = 16.2 kJ mol^{-1}; m_G (V_H), 12.0 kJ mol^{-1} M^{-1}. The experimentally determined *m*-values are in good agreement with the theoretically expected values (Myers *et al.*, 1995). The V_H domain is thus considerably less stable than the V_L domain. This difference in stability is particularly evident after normalization of the unfolding transitions to the fraction of unfolded protein (F_U) (Figure 2(c)). While the isolated V_L domain is still fully folded at 2 M GdmCl, the V_H domain is already unfolded under these conditions. It should be noted that this difference in stability is not a general feature of V_L and V_H domains, as the stability of both cover a wide range and depend on the molecular details of a particular domain, and the molecular features are only slowly emerging (Wörn & Plückthun, 2001).

Equilibrium unfolding of the scFv fragment was followed by the shift in the emission maximum

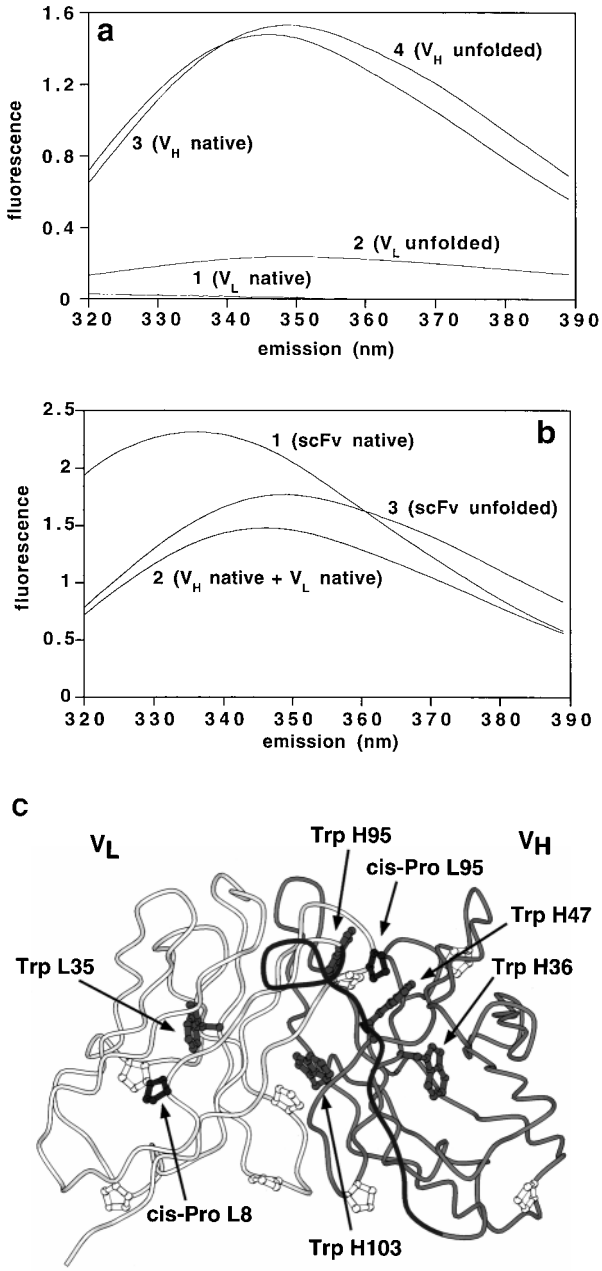

Figure 1. Fluorescence emission spectra of the scFv fragment and the isolated domains. (a) Native (spectrum 1) and unfolded V_L domain (spectrum 2), native (spectrum 3) and unfolded V_H domain (spectrum 4). (b) Native scFv fragment (spectrum 1), computational addition of the fluorescence emission spectra of native V_L and native V_H domain at a 1:1 stoichiometry (spectrum 2), unfolded scFv fragment (spectrum 3). Fluorescence intensities are given in arbitrary units, which were chosen such that the fluorescence of the native V_H domain at 1.0 μM was set to 1.0. Protein excitation was at 295 nm and the protein concentration was 1.0 μM, except for spectrum 1 shown in (a), where it was 3 μM. (c) Structure of the scFv fragment 4D5, based on the crystal structure of the Fv fragment (Eigenbrot *et al.*, 1993) and a modeled linker. The V_H domain is colored dark grey, the V_L domain light grey and the linker black. The side-chains of the tryptophan residues are shown in ball-and-stick representation (grey), while *trans* proline residues are shown in white and *cis* proline residues in black. The numbering is as described by Kabat *et al.* (1991).

(Δem_{max}) (Figure 2(d)), as well as by a global fit to the fluorescence intensities between 310 and 420 nm (Figure 2(e)) (Bilsel *et al.*, 1999; Gualfetti *et al.*, 1999). Two transitions are observable. The first transition (1.0 M GdmCl-1.9 M GdmCl) is characterized by a large shift in Δem_{max} from 336 nm to 346 nm. In the second transition (2.0-3.3 M GdmCl), there is only a small shift in Δem_{max} from 346 nm to 349 nm. As the change in emission maximum Δem_{max} is a probe that monitors the integrity of the heterodimer interface, we suggest that domain dissociation and unfolding of the V_H domain occurs in the first transition, whereas the still intact V_L domain unfolds in the second transition. This model of sequential domain unfolding is in agreement with previous proteolysis experiments (Wörn & Plückthun, 1998b). At 2 M GdmCl, the V_L domain is resistant to proteolysis, while the V_H domain is apparently unfolded and completely digested.

We also used a global fit of all intensities to a three-state model ($N \rightleftharpoons I \rightleftharpoons U$). However, because the spectral change in the second transition is very small, it is very difficult to unambiguously derive the free energies of the three-state equilibrium. Nevertheless, the values estimated from the global fit (about 33 and 31 kJ mol^{-1}, with *m*-values of about 23 and 14 kJ mol^{-1} M^{-1}) are consistent with the V_H domain being stabilized to about the level of the isolated V_L domain in the assembly, which is also reflected in its increased protection against deuterium exchange when in the complex compared to being in isolation (see below). Because of the different *m*-values, still two transitions are observed. Also, the *m*-value of the first transition is higher than the second (as expected for a higher cooperativity for the scFv than for the then isolated V_L domain). Finally, the second transition (interpreted as V_L unfolding) indeed has characteristics similar to those of the isolated V_L domain. These factors are consistent with the intermediate consisting of a native-like V_L domain and a denatured V_H domain. Figure 2(f) shows the expected species distribution as a function of denaturant concentration.

Multiphasic refolding kinetics of the V_L domain

Four fluorescence phases are resolvable in the refolding of the equilibrium-denatured V_L domain. Two phases are resolvable by manual mixing (~40 % of the total fluorescence amplitude) (Figure 3 and Table 1), another two phases are resolvable by stopped-flow mixing (Figure 3 (inset and Table 1)). Manual-mixing double-jump experiments (rapid unfolding of V_L in 6 M GdmCl for 20 seconds, followed by immediate refolding) (Schmid, 1986) reduces the amplitude of the two slow fluorescence phases by >90 % (data not shown). Independent experiments had shown that the unfolding rate of the V_L domain is about 0.7 s^{-1} under these conditions, such that only 0.00008 % of the native species is left after 20 seconds unfolding (data not shown). The slow

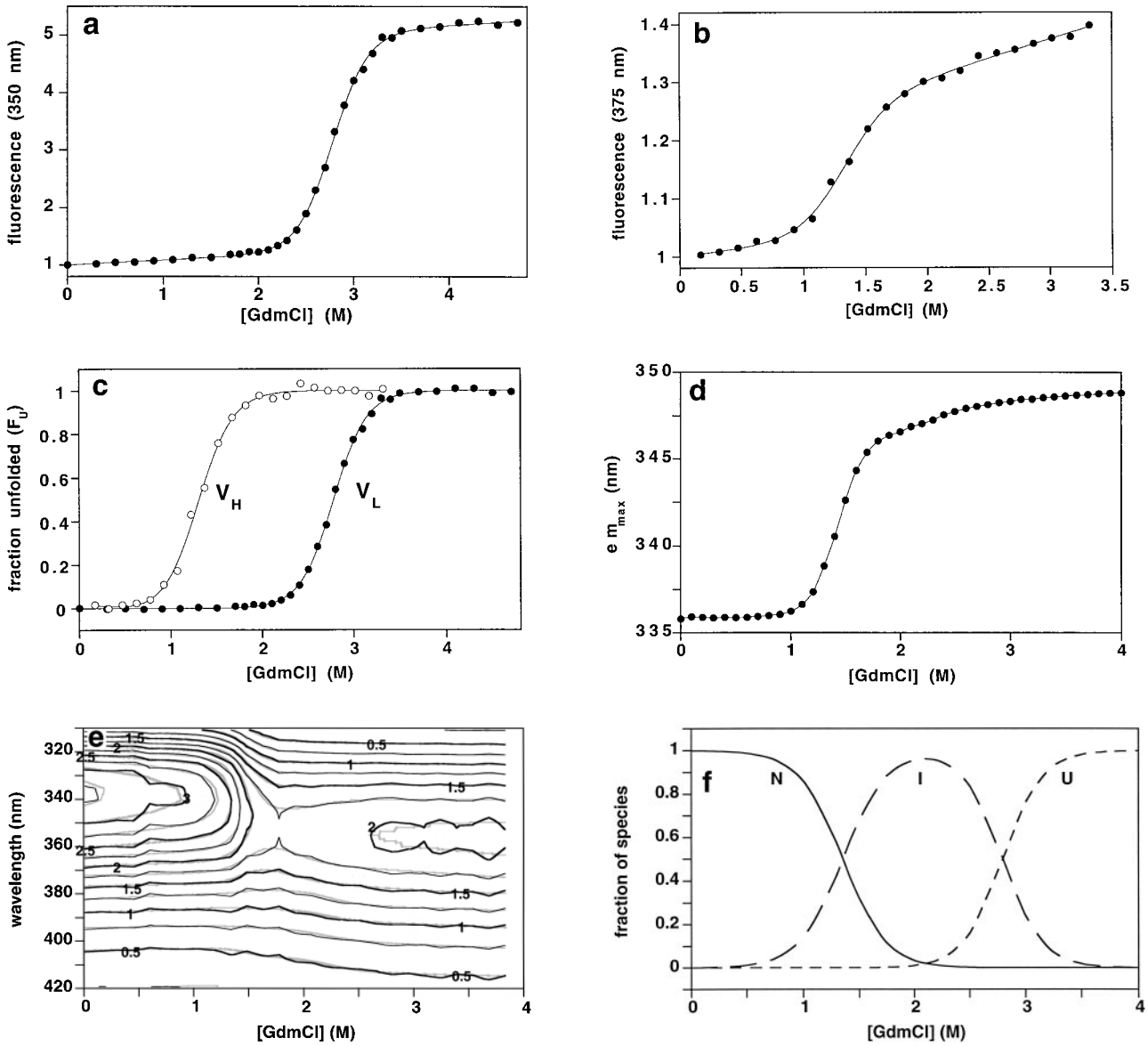

Figure 2. Equilibrium unfolding transition of the (a) V_L domain and (b) V_H domain. (c) Unfolding transitions of the V_L domain (filled circles) and the V_H domain (open circles) after normalization to the fraction of unfolded protein (F_U). The continuous lines in (a)-(c) are fit to a two-state unfolding reaction with the linear free energy model. (d) Equilibrium unfolding transition of the scFv fragment, monitored by the shift in the emission maximum. The continuous line is not a fit, but is supplied to guide the eye. Protein concentrations were 1.0 μM. (e) Contour plot of the unfolding transition of the scFv fragment. The experimental data are shown in black, the global fit to a three-state model using the program SAVUKA (Bilsel *et al.*, 1999; Gualfetti *et al.*, 1999) shown in grey lines. The numbers on the contour lines indicate fluorescence intensities. For details, see the text. (f) Distribution of the species according to the global fit in (e). The intermediate I is interpreted as native V_L linked to unfolded V_H. For details, see the text.

manual phases might therefore arise from slow proline *cis/trans*-isomerization in non-native states. The V_L domain contains two *cis*-prolines and five *trans*-proline residues (Eigenbrot *et al.*, 1993) (Figure 1(c)).

"Fast track" and "slow track" refolding in the V_L domain

To characterize the various refolding phases in the V_L domain, we next performed $^1H/^2H$-exchange protection experiments (Figure 4). Folding of the equilibrium-denatured and deuterated V_L domain was initiated by a 1:100 dilution into ^2H_2O buffer (p^{2}H 6.7), and allowed to proceed for various lengths of time. A further 1:10 dilution into ^1H_2O buffer (final pH 6.0) allowed refolding to go to completion and still unprotected ^2H to exchange for ^1H. A single peak is seen in the mass spectrum of the protonated V_L domain (peak maximum 12578 Da) (Table 2). If the denatured and fully deuterated V_L domain is folded to completion in ^2H_2O buffer, the mass shifts to 12,614 Da. This

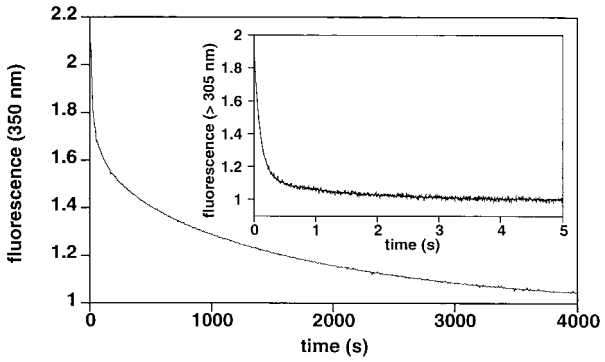

Figure 3. Refolding kinetics of the V_L domain. Shown are representative fluorescence traces, obtained by manual mixing and (inset) stopped-flow mixing. Reactions were followed by monitoring the change in fluorescence at 350 nm (manual mixing) or >305 nm (stopped-flow mixing). Protein concentrations were 2 μM.

indicates that 36 ^{2}H ions become trapped in the V_L domain during refolding. A refolding pulse of only 20 seconds in ^2H_2O results in bimodal mass spectra, indicative of the existence of two populations of molecules differing in the extent of stable and persistent structure. The higher molecular mass peak (~60-70 %) represents a native-like species (I_{native}), as the mass peak center (12,612 Da) is essentially that of the fully deuterated (native) sample (12,614 Da). The second peak shows a mass of 12,593 Da, which is between the native and the unfolded V_L domain. This peak must be attributed to a less-structured intermediate ($I_{non\text{-}native}$), with only 15 trapped ^{2}H ions. Longer folding times in ^2H_2O lead to a gradual decrease in the population of $I_{non\text{-}native}$, on a time-scale comparable to the fast fluorescence phase seen in the manual mixing experiment (rate constant: ~0.01 s^{-1}) (Figure 3). The rather slow disappearance of $I_{non\text{-}native}$, with a large fraction of I_{native} already present after ten seconds, rules out that this intermediate is a sequential intermediate, preceding the native-like species. Rather, it must be formed in a reaction competing with ''fast track'' folding into I_{native}. The very slow fluorescence phase (rate constant: 0.00072 s^{-1}) is not visible by ^{1}H/^{2}H-exchange, the consequence being that proline *cis/trans*-isomerization cannot involve major structural changes. Nevertheless, proline conformation does have a profound influence on the folding reaction of the scFv fragment, in that a correct Xaa-Pro peptide bond is required for productive domain interaction and formation of the native heterodimer interface (see below). Slow track folding is no longer detectable after short-term denaturation (Figure 4, lower spectra). Only a single peak with a peak maximum at 12,615 Da is seen in the earliest resolvable mass spectrum, indicating that under these conditions, full ^{1}H/^{2}H-exchange protection has been achieved in the deadtime of the manual mixing experiment (20 seconds).

The peak maximum of the single peak after short-term denaturation (12,615 Da) suggests that there must be considerable in-exchange of deuterons into the V_L domain within the 20 seconds refolding pulse in ^2H_2O buffer. Otherwise, the number of trapped ^{2}H ions should be reduced by

Table 1. Summary of the kinetic refolding data of the V_H and V_L domain and the scFv fragment

Protein	Refolding procedure[a]	[GdmCl] (M)[b]	k_f (s^{-1})[c]	Relative amplitude[d]
V_L	st. flow	0.16	10.2	0.86
			0.80	0.14
V_L	man. dil.	0.06	0.021	0.42
			0.00060	0.58
V_H	st. flow	0.08	0.22	0.61
			0.018	0.39
V_H (scFv)[e]	st. flow	0.08	0.21	0.72
			0.023	0.28
	man. dil.	0.02	0.24	0.76
			0.012	0.24
scFv[f]	man. dil. (eq. den.)	0.06	0.00069	1.0
		0.86	0.001	1.0
	man. dil. (sh. tm. den.)	0.06	0.0075	0.42
			0.00064	0.58
		0.86	0.016	0.89
			0.0011	0.11

[a] The refolding reaction was initiated either by stopped-flow mixing (st. flow) or by manual dilution (man. dil.).
[b] Final [GdmCl] in the refolding buffer.
[c] Refolding rate constants. If two rate constant are shown, the refolding reaction was biphasic and the fluorescence trace fitted to two exponentials. Errors were <5 %.
[d] Relative amplitudes of the refolding phases. The relative amplitudes refer to the experimentally resolvable amplitude, which was set to 1.0.
[e] Refolding of the denatured V_H domain from the equilibrium unfolding intermediate of the scFv fragment in 2 M GdmCl (native V_L domain, unfolded V_H domain).
[f] Refolding of the scFv fragment after equilibrium-denaturation (eq. den.) or short-term denaturation (sh. tm. den.) in 6 M GdmCl.

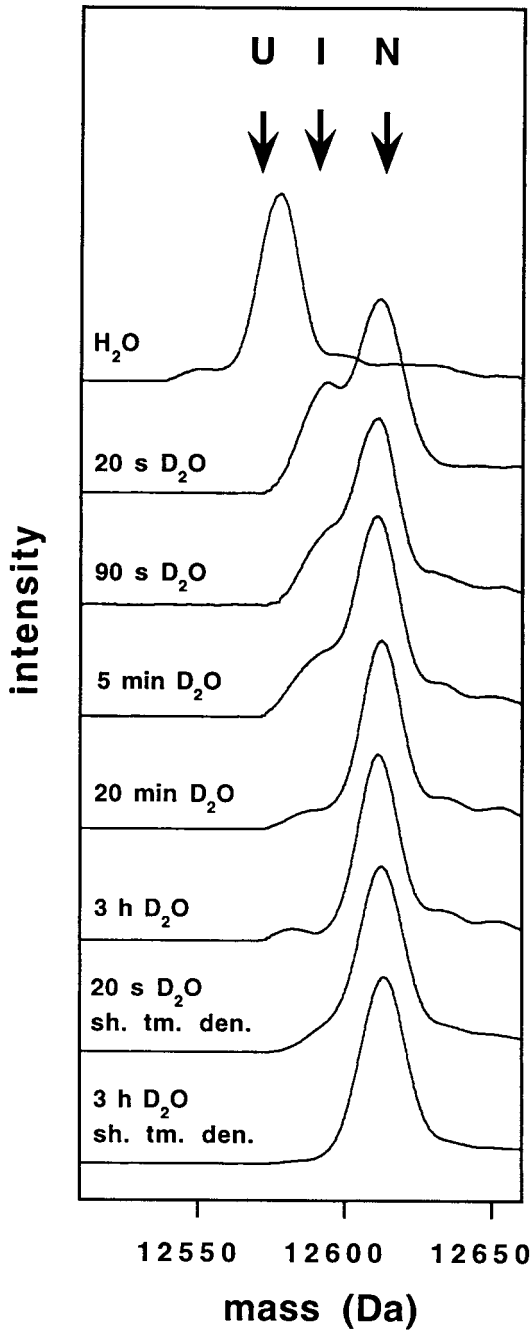

Figure 4. Refolding of the V_L domain, monitored by $^1H/^2H$-exchange and ESI-MS. The time labels indicate the refolding time in ^2H_2O buffer, before $^1H/^2H$-exchange was initiated by a 1:10 dilution into ^1H_2O buffer. Protein concentration after the first dilution step was 2 μM. Spectra obtained after short-term unfolding are labeled (sh. tm. den.).

about 25% ($36 \times 0.75 = 24$ ^2H), compared to the experiment with equilibrium-denatured protein, in order to account for the residual amount of 25% H_2O present during the short unfolding reaction. Such a back-exchange during the subsequent folding in ^2H_2O buffer is possible only if the rate of folding into an exchange-resistant conformation (k_{prot}) is slower than the rate of $^1H/^2H$-exchange at the p^2H used (6.7, not corrected for the isotope-effect). As the exchange rates for unprotected deuterons in random coils are known (Bai *et al.*, 1993), the upper limit for k_{prot} must be in the order of $\sim 10\ s^{-1}$.

Refolding kinetics of the V_H domain in the absence and presence of the V_L domain

Figure 5(a) illustrates the refolding kinetic trace of the isolated V_H domain. The refolding reaction was initiated by diluting the denatured protein (2 M GdmCl) in a stopped-flow apparatus (to 0.08 M GdmCl). The reaction was monitored by the change in fluorescence at >335 nm (Figure 1). Two kinetic phases are observed, with rate constants of $0.22\ s^{-1}$ (relative amplitude of 0.61) and $0.018\ s^{-1}$ (relative amplitude of 0.39) (Table 1). In an additional experiment, we investigated the folding of the V_H domain in the context of the scFv fragment. The reaction was started from the equili-

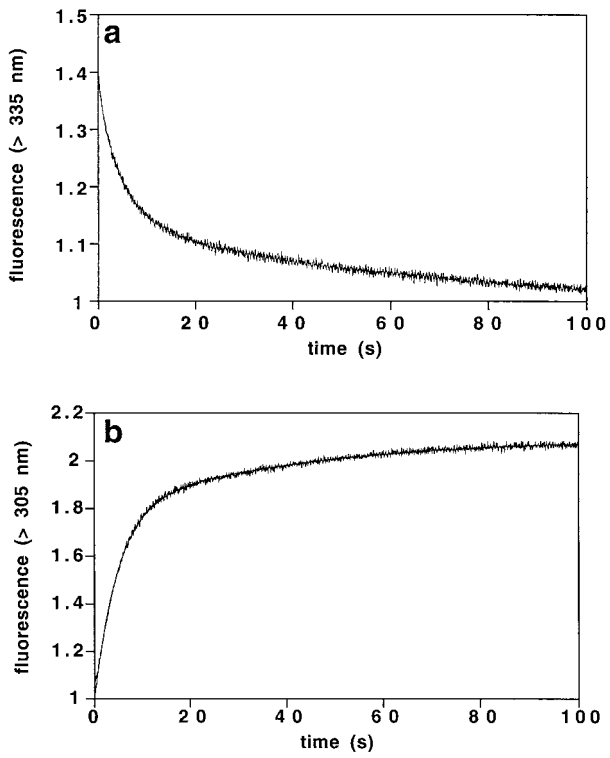

Figure 5. (a) Refolding of the isolated V_H domain. The reaction was followed by monitoring the change in fluorescence at > 335 nm. The fluorescence intensity is normalized to the calculated fluorescence at infinite time, which was arbitrarily set to 1.0. (b) Refolding of the V_H domain from the equilibrium unfolding intermediate of the scFv fragment (native V_L, unfolded V_H). The reaction was followed by monitoring the change in fluorescence at >305 nm. The fluorescence intensity is normalized to the fluorescence intensity at zero time, which was set to 1.0. Protein concentrations were 4 μM. Protein excitation was at 295 nm.

Table 2. Mass spectrometric analysis of the kinetic $^1H/^2H$-exchange experiments of the isolated domains V_L and V_H

Protein	Unfolding procedure[a]	Refolding time in ^2H_2O[b]	Mass (Da)[c]	Trapped deuterons[d]
V_L	-	-	12,578	0
V_L	eq. den.	20 s	12,593 ± 2	15 ± 1
			12,612 ± 1	34 ± 1
V_L	eq. den.	90 s	12,613 ± 1	35 ± 1
V_L	eq. den.	5 min	12,613 ± 1	35 ± 1
V_L	eq. den.	20 min	12,614 ± 1	36 ± 1
V_L	eq. den.	3 h	12,614 ± 1	36 ± 1
V_L	sh. tm. den.	20 s	12,613 ± 1	35 ± 1
V_L	sh. tm. den.	3 h	12,615 ± 1	37 ± 1
V_H	-	-	13,863	0
V_H	eq. den.	20 s	13,882 ± 3	19 ± 3
V_H	eq. den.	20 min	13,883 ± 3	20 ± 3
V_H	eq. den.	3 h	13,885 ± 2	22 ± 2
scFv[e]	eq. den.	20 s	26,742 ± 3	66 ± 3 (30 ± 3)[f]
scFv	eq. den.	20 min	26,743 ± 2	67 ± 2 (31 ± 2)
scFv	eq. den.	3 h	26,744 ± 2	68 ± 2 (32 ± 2)

[a] The protein was either equilibrium-denatured (eq. den.; >12 hours in 6 M GdmCl/^2H_2O) or short-term denatured (sh. tm. den.; 20 seconds in 6 M GdmCl/^2H_2O), before the refolding reaction was initiated by a manual 1:100 dilution into ^2H_2O buffer. Final [GdmCl] was 0.06 M.

[b] Refolding time in ^2H_2O buffer before the $^1H/^2H$-exchange reaction was initiated by a manual 1:10 dilution into ^1H_2O-buffer.

[c] Experimentally determined masses of the peak maxima. If two masses are reported, the masses refer to the mass of the folding intermediate and the native-like V_L domain, respectively.

[d] Number of stable deuterons in the refolded protein.

[e] The $^1H/^2H$-exchange reaction was initiated from the equilibrium-denatured state in 2 M GdmCl. Final [GdmCl] was 0.1 M. The equilibrium-unfolding intermediate was prepared by a 1:3 dilution of the fully denatured and deuterated scFv fragment (20 mM Mops (p^2H 6.7), 6 M GdmCl) in 20 mM Mops (p^2H 6.7). For details see Materials and Methods.

[f] The values in parentheses represent the number of deuterons in the scFv fragment after subtracting the deuterons found in the V_L domain, refolded to completion in ^2H_2O.

brium unfolding intermediate at 2 M GdmCl, i.e. under conditions where the V_L domain is still native, while the V_H domain is already denatured (Figure 2) (Wörn & Plückthun, 1998b). The reaction progress was monitored by the change in fluorescence at > 305 nm. This experiment thus monitors the refolding kinetics of the V_H domain indirectly by measuring the large fluorescence increase upon domain association and formation of the native interface (Figure 1(b)). The increase in fluorescence fits to a double exponential and rate constants of 0.21 s^{-1} (relative amplitude of 0.72) and 0.023 s^{-1} (relative amplitude of 0.28) were obtained. It can be seen that the rate constants and relative amplitudes do not differ significantly from those obtained with the isolated V_H domain, the consequence being that the same folding reaction, namely folding of the V_H domain, is rate determining in the two experiments. This means that covalently linking the two domains into an scFv fragment does not affect the refolding kinetics of the V_H domain to a measurable extent.

Manual mixing experiments on a longer timescale (0-600 seconds) ruled out the presence of an additional slow phase, which might have escaped detection in the stopped-flow experiment (Table 1) (data not shown). However, the rate constant of the slow refolding phase was slightly smaller in this experiment (0.01 s^{-1}). This minor difference may be due to the fact that in the manual mixing experiments, the reaction was followed at a fixed emission wavelength (326 nm), whereas the stopped-flow reaction was monitored with a cut-off filter (>305 nm).

Stabilization of the V_H domain in the scFv fragment

Above, we showed that the presence of the native V_L domain does not affect the refolding kinetics of the V_H domain. Despite the passive role in refolding of the V_H domain, we now show that the V_L domain stabilizes the V_H domain in the scFv heterodimer, consistent with the interpretation of the global fit data of the scFv equilibrium unfolding. Figure 6(a) shows the time-course of $^1H/^2H$-exchange protection in the V_H domain in the scFv-context after refolding from the equilibrium-denatured state (2 M GdmCl). In this experiment, the scFv fragment was first unfolded and completely deuterated in 6 M GdmCl. The scFv fragment was then diluted into 2 M GdmCl/^2H_2O buffer to allow folding of the V_L domain to go to completion, whereas the V_H domain remains unfolded under these conditions (Figure 2). Finally, folding of the V_H domain was triggered by dilution of the scFv-intermediate into ^2H_2O buffer, followed by $^1H/^2H$-exchange in ^1H_2O buffer as described in detail for the isolated V_L domain. The number of trapped ^2H ions in the scFv fragment at quenching time t is thus the sum of trapped ^2H ions in the V_L domain (36 ^2H) plus the number of exchange-resistant ^2H ions trapped in the V_H domain at quenching time t. It was found that there is essentially no difference in the number of protected ^2H

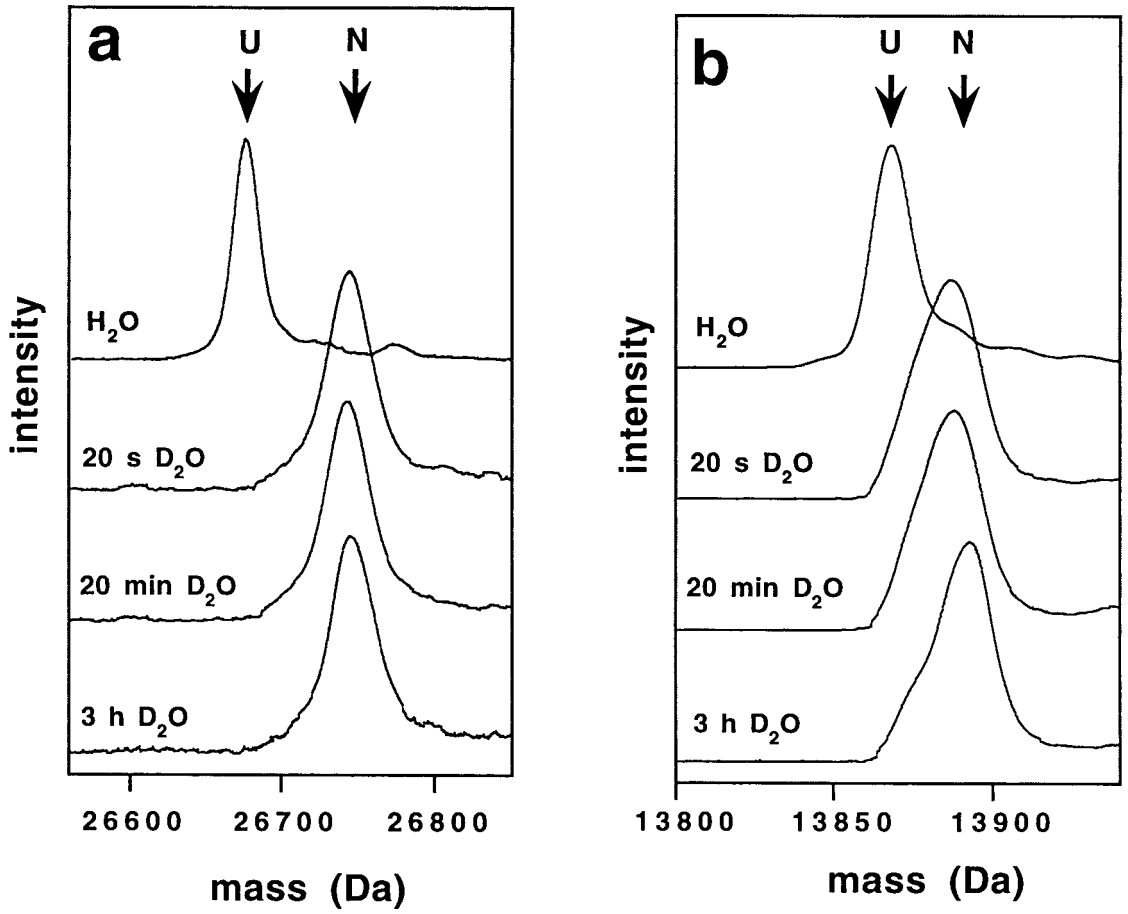

Figure 6. (a) Refolding of the V_H domain monitored by $^1H/^2H$-exchange and ESI-MS after refolding from the equilibrium unfolding intermediate of the scFv fragment (2 M GdmCl). (b) Refolding of the isolated V_H domain from 2 M GdmCl, monitored by $^1H/^2H$-exchange and ESI-MS. Time labels indicate the refolding time in ^2H_2O buffer, before the $^1H/^2H$-exchange reaction was quenched by a 1:10 dilution into ^1H_2O buffer.

ions in the scFv fragment between the earliest and last mass spectrum obtained (Table 2). Maximal $^1H/^2H$-exchange protection is therefore accomplished in the deadtime of the experiment. In total, 70 ^2H ions are trapped in the scFv fragment. Subtracting the 36 ^2H ions in the isolated V_L domain, this leaves 34 trapped ^2H ions in the V_H domain. In the isolated V_H domain, only 22 ^2H ions are trapped (see below). $^1H/^2H$-exchange-protection is thus equally distributed among the two domains in the scFv fragment, as long as they form a complex. The exchange-resistant core of the V_H domain, which lacks *cis*-proline residues, must thus be formed in the deadtime of the experiment (20 seconds), i.e. on the time-scale of the fast stopped-flow phase, or before. The slow fluorescence phase, on the other hand, cannot involve major structural changes. Otherwise, part of the $^1H/^2H$-exchange protection kinetics should be resolvable by manual mixing, as the intrinsic exchange rate at pH 6.0 is about 1 s^{-1}, and thus two orders of magnitude faster than the rate constant of the slow phase (0.01 s^{-1}).

Repeating the experiment with the isolated V_H domain gave qualitatively comparable results (Table 2 and Figure 6(b)). Again, maximal exchange-protection was detectable within the deadtime of the manual mixing experiment, but only 22 ^2H ions become trapped during refolding. The peaks are rather broad, which suggests the presence of a population of species, differing slightly in the number of exchange-protected ^2H. It is rather unlikely that the lower exchange-protection of the isolated V_H domain is due to incomplete folding or aggregation. In such a case, one would not expect identical rate constants and relative amplitudes in the fluorescence refolding experiments with the isolated and scFv-constituting V_H domains. In the light of the rather low thermodynamic stability of this isolated V_H domain, a more plausible explanation is that the V_H domain becomes stabilized in the context of the scFv fragment (Wörn & Plückthun, 1998b, 2001), thereby reducing $^1H/^2H$-back-exchange from locally and globally unfolded states.

Early domain interaction in the scFv fragment

No stopped-flow phases are detectable in the refolding of the equilibrium denatured scFv frag-

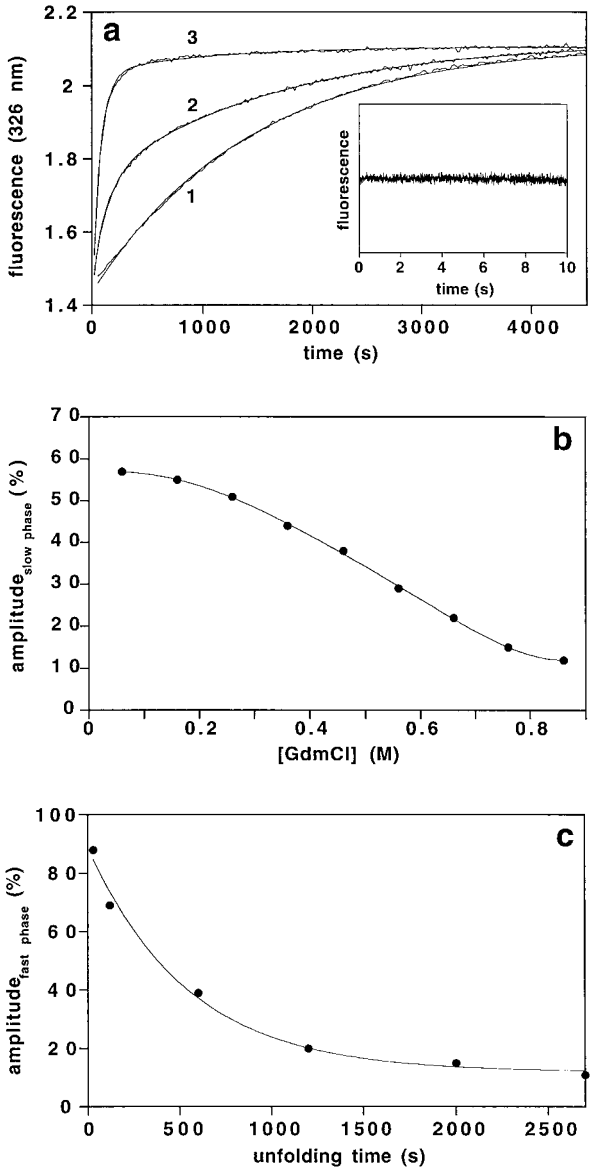

Figure 7. (a) Refolding of the scFv fragment monitored by Trp-fluorescence after equilibrium-denaturation (trace 1) and short-term denaturation (trace 2 (in 0.06 M GdmCl), trace 3 (in 0.086 M GdmCl)). Reactions were monitored by following the change in fluorescence at 326 nm. Protein excitation was at 295 nm. Fluorescence intensities are normalized to the fluorescence of the denatured protein, arbitrarily set to 1.0. (b) Dependence of the amplitude of the slow phase on [GdmCl] in the refolding buffer. Short-term denatured scFv fragment was unfolded for the indicated time and diluted into 0.86 M GdmCl to initiate refolding. (c) Plot of the relative fraction of the slow folding amplitude *versus* the unfolding time in 6 M GdmCl.

ment (Figure 7(a), insert). This requires that both domains interact within the deadtime of the experiment (~2 ms). If they did not interact, an algebraic sum of the folding of the V_H and V_L domain, both of which show a fluorescence decrease (Figures 3 (inset) and 5(a)), should be seen. An early domain interaction is also supported by the manual mixing experiments. The trace of the fluorescence intensity at 326 nm, which monitors the formation of the native interface, starts from a value significantly higher (~40 %) than that of the unfolded heterodimer (Figure 7(a), trace 1, and Table 1). Therefore, we must postulate an additional burst phase in which the fluorescence intensity increases from that of the unfolded scFv fragment to the first observable time-point. The fluorescence intensity increases from this burst-phase level in a slow mono-exponential reaction. The rate constant of this reaction (0.00064 s^{-1}) is comparable to that of the very slow, proline-limited phase in the refolding of the isolated V_L domain (0.00089 s^{-1}).

Fast proline *cis/trans*-reisomerization in a folding intermediate of the scFv fragment

The above experiment suggests that proline *cis/trans*-isomerization is not only rate-limiting for the folding of the isolated V_L domain, but also rate-limiting in the assembly of the scFv fragment. To further support that hypothesis, we next performed a double-jump experiment (Schmid, 1986). Unfolding of the scFv fragment was achieved in 6 M GdmCl, which leads to complete unfolding in less than 20 seconds at 10 °C (data not shown, at most 5-8 % native species are predicted under these conditions from the unfolding rates reported by Ramm *et al.*, 1999). Refolding of short-term denatured scFv fragment (20 seconds in 6 M GdmCl) is biphasic (Figure 7(a), trace 2, and Table 1). About 40 % of the amplitude was gained in a fast phase (rate constant of 0.0075 s^{-1}). The remaining amplitude was established in a slow phase with an essentially unchanged rate constant (0.00064 s^{-1}). This indicates that the slow phase is still rate-limited by proline *cis/trans*-isomerization, despite the fact that the refolding reaction was initiated after short-term denaturation, i.e. with all proline residues in the native conformation.

Increasing GdmCl concentrations in the refolding buffer leads to a sigmoidal decrease in the amplitude of the slow, proline-limited phase (Figure 7(b)). At 0.86 M GdmCl, the highest concentration where the scFv fragment is still native (Figure 2(d)), the slow phase contributes only ~10 % to the total fluorescence increase (Figure 7(a), trace 3). Notably, the rate constants of both slow phases increase when going from 0.06 M GdmCl to 0.86 M GdmCl, the faster phase from 0.0075 s^{-1} to 0.16 s^{-1}, the slower phase from 0.00069 s^{-1} to 0.001 s^{-1} (Table 1).

Unfolding times longer than those required for complete denaturation of the scFv fragment (longer than 20 seconds) result in a gradual reappearance of the slow, proline-limited phase at the cost of the fast phase (Figure 7(c)). The build-up of the slow phase (rate constant of 0.0017 s^{-1}) is as expected, as the proline residues, which are in the native conformation immediately after fast unfolding, slowly begin to isomerize and reach their thermodynamic

cis/trans-equilibrium. However, it is noteworthy that the apparent rate constant of the *cis/trans*-isomerization reaction (0.0017 s^{-1}) in 6 M GdmCl is too small to explain the high fraction of slowly folding species observable after short-term unfolding and refolding under strongly native conditions (0.06 M GdmCl), as only a negligible fraction of the native proline residues would be able to isomerize within the brief unfolding pulse (20 seconds) in 6 M GdmCl. Therefore, proline *cis/trans*-isomerization has to take place spontaneously in a folding intermediate, rather than the denatured state, and at a rate significantly faster than the apparent rate of isomerization in the denatured protein under strongly denaturing conditions (6 M GdmCl). Higher GdmCl concentrations seem to prevent proline *cis/trans*-reisomerization in the folding intermediate, as indicated by the increase in the fast fluorescence phase. In other words, more destabilizing refolding conditions lead to apparently faster domain assembly into the native scFv fragment.

^{1}H/^{2}H-exchange kinetics of the scFv fragment

During the time-course of folding, 73 ^{2}H ions are incorporated into the scFv fragment (Figure 8(a) and Table 3). The mass spectrum at 20 seconds shows a peak maximum at 26,696 Da. Thus, only 22 ^{2}H deuterons are trapped in the scFv fragment at this stage, a number well below the sum of ^{2}H ions trapped in the two isolated domains after an identical refolding time in ^2H_2O (34-53 ^{2}H, depending on whether $I_{non\text{-}native}$ or I_{native} of the V_L domain is considered for the calculation). The low exchange protection in the scFv fragment means that the two domains do not refold independently in the linked heterodimer. Rather, they must interact prematurely early in folding, before full ^{1}H/^{2}H-exchange protection can be established in the constituting domains. It is tempting to speculate that the non-native domain interaction shown here is also manifest as the burst-phase amplitude in the manual fluorescence refolding experiment (Figure 7(a)).

Except for the fast formation of the weakly structured intermediate, formed in the deadtime of the experiment, subsequent protection of ^{2}H ions from exchange with solvent was slow enough to be resolved by manual mixing techniques (Figure 8(c)). About 85 % of the ^{2}H ions are trapped in a very slow phase with a rate constant (0.0004(±0.0001) s^{-1}), which is comparable to the rate of the proline *cis/trans*-isomerization phase seen in the fluorescence experiment (0.00069(±0.0001) s^{-1}). Only ~15 % are trapped in a significantly faster phase (rate constant: 0.021(±0.023) s^{-1}).

Interestingly, premature domain association is also observed after short-term denaturation (Figure 8(b)). A total of 26 ^{2}H ions are trapped in the scFv fragment after short-term denaturation. This is only insignificantly higher than the 22 ^{2}H ions trapped at identical time after equilibrium denaturation. On the other hand, essentially full exchange protection (~70 ^{2}H) would be expected, if the domain did fold independently before assembling into the heterodimer. Again, the gain in full exchange-protection is slow enough to be resolved by manual mixing. About 65 % are protected in a fast phase (rate constant of 0.021(±0.004) s^{-1}), whereas only 35 % are trapped in the slow phase (rate constant of 0.0011(±0.0003) s^{-1}). Therefore,

Table 3. Mass spectrometric analysis of the kinetic ^{1}H/^{2}H-exchange experiments of the scFv fragment

Unfolding procedure[a]	Refolding time in ^2H_2O[b]	Mass (Da)[c]	Trapped deuterons[d]
-	-	26,674	-
eq. den.	20 s	26,696 ± 2	22 ± 2
eq. den.	90 s	26,701 ± 2	26 ± 2
eq. den.	5 min	26,701 ± 2	27 ± 2
eq. den.	20 min	26,706 ± 2	32 ± 2
		26,746 ± 3	72 ± 3
eq. den.	40 min	26,746 ± 2	72 ± 2
eq. den.	90 min	26,747 ± 2	73 ± 2
eq. den.	3 h	26,748 ± 2	74 ± 2
sh. tm. den.	20 s	26,700 ± 3	26 ± 3
sh. tm. den.	90 s	26,703 ± 3	29 ± 3
		26,739 ± 3	65 ± 3
sh. tm. den.	5 min	26,740 ± 4	66 ± 4
sh. tm. den.	20 min	26,742 ± 3	68 ± 3
sh. tm. den.	40 min	26,745 ± 2	71 ± 2
sh. tm. den.	90 min	26,745 ± 2	71 ± 2
sh. tm. den.	3 h	26,746 ± 3	72 ± 3

[a] The protein was either equilibrium-denatured (eq. den.; >12 hours in 6 M GdmCl/^2H_2O) or short-term denatured (sh. tm. den.; 20 seconds in 6 M GdmCl/^2H_2O), before the refolding reaction was initiated by a manual 1:100 dilution into ^2H_2O buffer

[b] Refolding time in ^2H_2O buffer before the ^{1}H/^{2}H-exchange reaction was initiated by a manual 1:10 dilution into ^1H_2O buffer.

[c] Experimentally determined masses of the peak maxima. If two peak masses are reported, the masses refer to the mass of the folding intermediate and the native-like scFv fragment, respectively.

[d] Number of stable deuterons in the refolded protein.

the outcome of the $^1H/^2H$-exchange protection reflects at least qualitatively the results obtained with fluorescence spectroscopy.

Discussion

Equilibrium unfolding of the scFv fragment and the domains V_H and V_L

Two extreme cases are possible to describe equilibrium unfolding of a heterodimeric protein (Brandts *et al.*, 1989; Ramsay & Freire, 1990). At one extreme, the domains unfold as independent entities, which exhibit the same intrinsic thermodynamic stability, irrespective of whether they are part of the heterodimer or present in isolated form. At the other extreme, the domains stabilize each other to such an extent that the thermodynamic stability of the heterodimer exceeds that of either of the domains, meaning that interface dissociation and domain unfolding are coupled events. In the first case and in intermediate cases, an equilibrium unfolding intermediate can exist with one folded and one unfolded domain. When the coupling is significant, one domain profits from the other, more stable one and unfolds at higher denaturant concentrations than when in isolation, but still earlier than the more stable one. These models have recently been summarized for antibody fragments (Wörn & Plückthun, 1999, 2001). The results presented here, together with previous experiments (Wörn & Plückthun, 1998a; Ramm *et al.*, 1999), indicate that the scFv fragment 4D5 belongs to the category with a stable intermediate (Figure 9(a)). The less stable V_H domain unfolds first, giving rise to a stable equilibrium unfolding intermediate.

Refolding of the V_L domain

The refolding of the V_L domain occurs in two parallel pathways (Figure 9(b)). About 60-70 % of the equilibrium-denatured ensemble (U_L) folds rapidly (<20 seconds) *via* a fast track into a compact intermediate (I_{native}), with native-like $^1H/^2H$-exchange protection, but with one (or more) non-native proline residues. At present, we simplify the model, in that I_{native} is formed directly from the denatured ensemble in a single reaction, and we cannot rule out the existence of additional, kinetically unresolved intermediates in the dead-time of the experiment (20 seconds). Future $^1H/^2H$ -exchange experiments on a shorter time-scale and stopped-flow fluorescence experiments at a wider range of GdmCl concentrations should clarify this question. Proline *cis/trans*-isomerization is rate-limiting for the formation of the native protein (N_L) and must occur in I_{native}.

From the similarity between the relative weight of the major stopped-flow amplitude on the total fluorescence amplitude (0.6-0.7) and the relative weight of I_{native} on the total mass peak area at 20 seconds (0.6-0.7), it is tempting to propose that I_{native} is formed in the faster of the two stopped-flow reactions (rate constant 10.2 s^{-1}). This hypothesis is reasonable, as the decrease in Trp-fluorescence, observable in the stopped-flow experiment, requires that the core-TrpL36 must become juxtaposed to the conserved disulfide bond, which can be achieved only if the native folding topology is developed simultaneously.

The remaining 30-40 % of equilibrium-denatured molecules fold *via* a slow track. First, an intermediate ($I_{non\text{-}native}$) is formed within the deadtime of the $^1H/^2H$-exchange experiment (20 seconds). $I_{non\text{-}native}$ is significantly less structured than I_{native}, with only 15 ^2H ions trapped in an exchange-resistant conformation. Native $^1H/^2H$-exchange protection in $I_{non\text{-}native}$ is on a time-scale comparable to that of the fast manual fluorescence phase (rate constant: ~0.02 s^{-1}), and thus still significantly faster than the very slow proline-phase (rate constant 0.00072 s^{-1}), detectable in the same experiment. $I_{non\text{-}native}$ is no longer populated after short-term denaturation, the consequence being that $I_{non\text{-}native}$ must be favored by non-native proline peptide bonds. Taking into account the high content of proline residues in the V_L domain (two *cis* proline, five *trans* proline residues) and assuming an average *cis/trans*-ratio of 0.1-0.2 for each proline-peptide bond under equilibrium unfolding conditions (Huyghues-Despointes *et al.*, 1999), the fraction of V_L molecules with exclusively native proline-peptide bonds should be extremely small, probably well below 10 %. In other words, more than 90 % of the equilibrium-denatured ensemble carries at least one incorrect proline residue. Since not 90 %, but only 30-40 % of all molecules fold into $I_{non\text{-}native}$, only a sub-population of denatured V_L molecules with non-native proline residues take the slow folding track. A plausible hypothesis is that this sub-population are those molecules with proline L8 and L95 *in trans*. Ongoing stopped-flow and $^1H/^2H$-exchange experiments will clarify the question of whether $I_{non\text{-}native}$ is a genuine on-pathway folding intermediate or a reversibly formed off-pathway dimer or microaggregate, favored at higher protein concentrations.

Refolding of the V_H domain

The refolding of the V_H domain was studied in two different experiments. First, refolding of the isolated V_H domain was studied by monitoring a small decrease in intrinsic Trp-fluorescence (Figure 9(c), Scheme 1). Second, refolding of the V_H domain was studied indirectly (Figure 9(c), Scheme 2). In this experiment, the folding reaction was initiated from the equilibrium unfolding intermediate of the scFv fragment, populated at 2 M GdmCl. This study, and earlier proteolysis experiments (Wörn & Plückthun, 1998b), show that in this intermediate, the V_L domain is still native, while the V_H domain is unfolded. Folding of the V_H domain was monitored by a large fluorescence increase upon interface formation. Interestingly, both experiments show biphasic kinetics, with similar rate constants

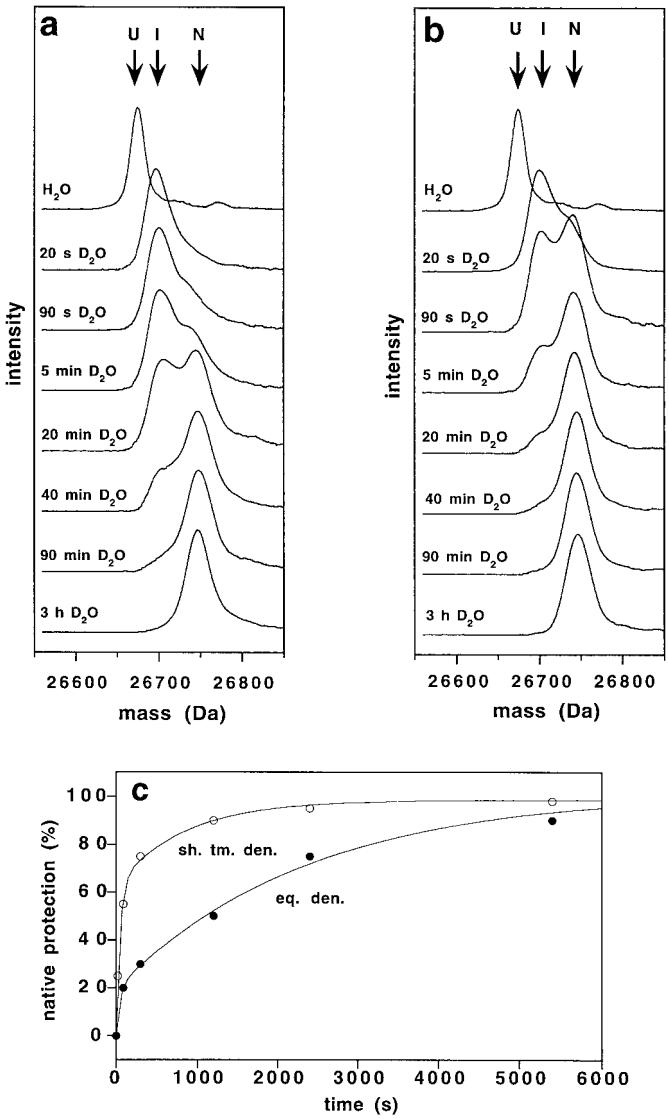

Figure 8. Refolding of the scFv fragment, monitored by $^1H/^2H$-exchange and ESI-MS. (a) Equilibrium-denatured scFv fragment. (b) Short-term denatured scFv fragment. The time labels indicate the refolding time in ^2H_2O buffer, before $^1H/^2H$-exchange was initiated by a 1:10 dilution into ^1H_2O buffer. (c) Kinetics of formation of the scFv fragment with native $^1H/^2H$-exchange protection after equilibrium denaturation (●) and short-term denaturation (○). The relative weight of the native protein at each time-point was determined from the ratio of the mass peak heights.

and relative amplitudes. $^1H/^2H$-exchange experiments show that full $^1H/^2H$-exchange protection is gained within the deadtime of the manual mixing experiment (20 seconds), the consequence being that the exchange-protected core is formed in the fast phase, or before.

The biphasic folding kinetics can be explained by a sequential or parallel folding model. In the sequential model (Figure 9(c), Schemes 1 and 2), the first phase monitors the formation of an intermediate with native-like $^1H/^2H$-exchange protection. This reaction is manifested by a fluorescence decrease in the isolated V_H domain ($U_H \rightarrow I_H$, scheme 1). A net fluorescence increase with comparable rate constants and relative amplitudes is seen in the scFv fragment, as the fluorescence increase upon the subsequent fast domain assembly outweighs the decrease in intrinsic fluorescence in the V_H domain (N_L-$I_{H\ (diss.)} \rightarrow N_L$-$I_{H\ (ass.)}$, scheme 2) and N_L-$I_{H\ (diss.)}$ never accumulates, but reacts in a fast reaction to N_L-$N_{H\ (ass)}$. The slower phase monitors the isomerization of this structured intermediate into the native protein ($I_H \rightarrow N_H$, Scheme 1; N_L-$I_{H\ (ass)} \rightarrow N_L$-$N_{H\ (ass)}$, Scheme 2).

In the parallel folding model, the fast phase would monitor the folding of the V_H domain into the native protein. The slow phase monitors the interconversion of a structured intermediate, formed in parallel with the fast folding reaction, into the native protein. Both of these reaction are manifested as a fluorescence decrease in the folding of the isolated V_H domain ($U_H \rightarrow N_H$;

$I_H \rightarrow N_H$, Scheme 3). In the scFv fragment, starting from the N_L-U_H state (Scheme 4), both reactions, N_L-$U_H \rightarrow N_L$-$N_{H\ (diss.)}$ and N_L-$U_H \rightarrow N_L$-$N_{H\ (diss.)}$ are visible indirectly as an increase in fluorescence that is actually caused by the reaction N_L-$N_{H\ (diss.)} \rightarrow N_L$-$N_{H\ (ass.)}$ which is fast and occurs immediately upon formation of N_L-$N_{H\ (diss.)}$.

From the available data, it is impossible to distinguish between the two models. The sequential folding model requires that the intermediate I_H stably interact with the V_L domain. Clearly, further experiments will be required to characterize the exact nature of these intermediates.

The refolding pathway of the scFv fragment

The refolding of the scFv fragment is summarized in Figure 9(d). Fluorescence spectroscopic and $^1H/^2H$-exchange experiments confirmed that the constituting domains of the scFv fragment do not refold independently after equilibrium-denaturation in 6 M GdmCl. The key observation is that significantly fewer exchange-protected ^2H are detectable in the scFv fragment at the earliest time-point resolvable by manual mixing than in the two isolated domains at identical time-points. An intermediate with physically not interacting, yet native-like domains (I_{open}) would have been expected from the behavior of the independent domains, if they folded independently. However, this is not formed to any measurable extent during the refolding of the heterodimer (crossed-out arrows). Rather, the two domains first associate quantitatively and prematurely before full $^1H/^2H$-exchange protection can be gained on the level of the domains (thick arrows). We call the intermediate with non-native domain contacts I_{trap} to account for the fact that the $^1H/^2H$-exchange protection kinetics is slowed in the heterodimer with respect to the isolated domains. When are these non-native contacts formed in the heterodimer? Stopped-flow experiments indicate that the fast refolding phases of the isolated domains are completely absent from the scFv fragment. Thus, the two domains may already interact in the deadtime of the instrument (2 ms). I_{trap} might, therefore, be formed with a rate constant >1000 s^{-1} or even faster.

It should be noted that in the reaction starting from N_L-U_H (Figure 9(c), Scheme 4) the trap is not formed, as the V_L domain is native all the time. For trap formation, at least V_L and probably both domains need to be non-native.

A detailed analysis of the time-course of the $^1H/^2H$-exchange protection experiment reveals that native exchange protection in the scFv fragment is gained in two phases. In the equilibrium-denatured protein, most of the deuterons (85(±6) %) become protected in a very slow phase. Notably, the estimated rate constant of this phase (0.00042(±0.0001) s^{-1}) is in good agreement with the rate constant of the slow, proline-limited fluorescence phase (0.00069 s^{-1}) that leads to the formation of the native heterodimer interface. In other words, the disappearance of I_{trap} seems to be kinetically coupled to proline *cis/trans*-isomerization reaction.

Under the conditions of the present experiments, I_{trap} is also quantitatively formed after short-term denaturation (starting from U_{cis}). Interestingly, the gain in native $^1H/^2H$-exchange protection is still biphasic and resolvable by manual mixing. This is in strong contrast to the isolated domains, where full $^1H/^2H$-exchange protection is established within the deadtime of manual mixing. The faster of the two protection phases (about 0.01 s^{-1}, relative weight 0.65(±0.05)) could be assigned to those molecules that escape from $I_{trap(cis)}$ with the proline residues in native conformation, as this phase is absent after equilibrium-denaturation. In contrast, the minor slow phase (relative weight 0.35 ± 0.05)) represents the population of molecules where proline *cis/trans*-reisomerization occurs before escaping from I_{trap} and rapidly folding into the native state. These molecules are trapped in the low protection conformation until proline residue *cis/trans*-isomerization allows folding into the native heterodimer.

After short-term denaturation, the molecules are believed to be in slow, proline *cis/trans*-isomerization limited equilibrium between $I_{trap(trans)}$ and $I_{trap(cis)}$ (see below), and escape only whenever the latter converts to $I_{open(cis)}$. Therefore, $I_{trap(trans)}$ would be a classical off-pathway intermediate in the double-jump experiment, while it would be on-pathway in the refolding of the equilibrium-denatured protein. We believe that the reaction $I_{trap(trans)}$ to $I_{open(trans)}$ does not take place to any appreciable extent for this antibody, for the following reason. The I_{open} species are the first in the pathway to have full proton protection (they must be as stable as the unlinked domains, which do show stable protection). The observed appearance of any species with native-like protection is, however, about 20-fold slower for the reaction starting from U_{trans} than from U_{cis} and occurs about at the rate of proline *cis/trans*-isomerization. This means that any formation of $I_{open(trans)}$ from $I_{trap(trans)}$ would either have to occur at that rate (or even more slowly or maybe not at all, as the reaction can go from $I_{trap(trans)}$ *via* $I_{trap(cis)}$ to $I_{open(cis)}$). In either case, protection would be obtained with the rate of proline *cis/trans*-isomerization, to facilitate this interconversion.

The relative weight of the persistent slow phase after short-term denaturation is determined by the ratio of proline *cis/trans*-reisomerization in I_{trap}, and the escape from I_{trap}. As the partitioning is about 1:1, the rates must be comparable. Why proline *cis/trans*-reisomerization is faster in I_{trap} than in the more extensively unfolded denatured ensemble (6 M GdmCl) remains to be shown. Possibly, the structured environment in I_{trap} accelerates the isomerization reaction by stabilizing the transition state and/or the ground state may be incompatible with a *cis*-proline. These structural features might be disrupted in the more extensively denatured

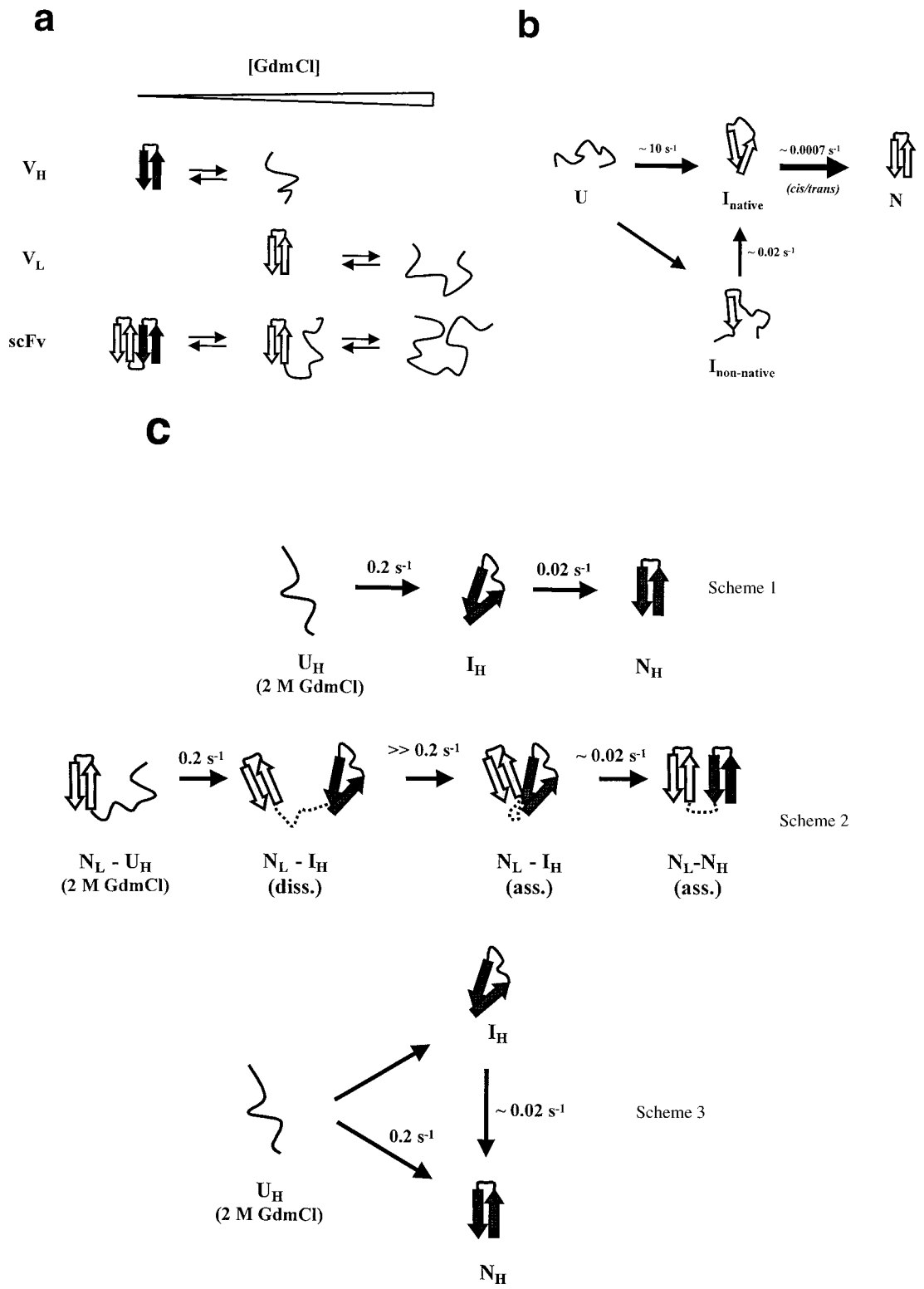

Figure 9 (*legend opposite*)

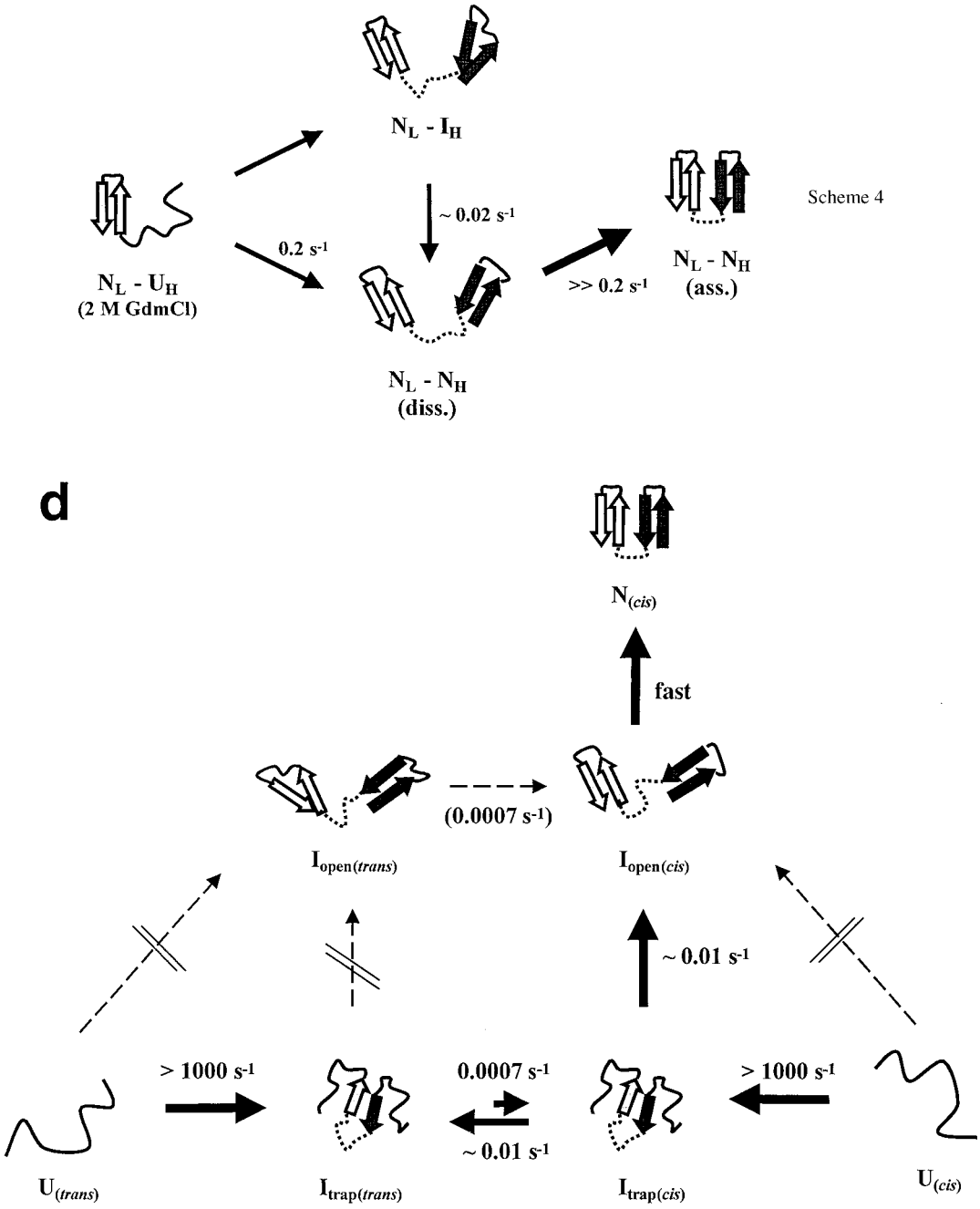

Figure 9. (a) Schematic depiction of the equilibrium unfolding behavior of the scFv fragment and the domains V_H and V_L as a function of denaturant concentration. (b) Refolding of the V_L domain. (c) Refolding of the V_H domain. Schemes 1 and 3, folding of isolated V_H domains; Schemes 2 and 4, folding of V_H as part of the scFv fragment; Schemes 1 and 2, sequential model; Schemes 3 and 4, parallel model. (d) Refolding of the scFv fragment. The extent of structure is symbolized by grey (V_L domain) and dark-grey arrows (V_H domain). The flux of material is represented by the thickness of the black arrows. The crossed-out arrow symbolizes that this direct step is not taking place. For further details, see the text.

protein at 6 M GdmCl, thereby slowing the apparent rate of proline *cis/trans*-isomerization. Denaturant-induced local unfolding of I_{trap} may also explain why higher GdmCl concentrations lead to an increase in the relative weight of the fast fluorescence phase, in other words, why the reaction becomes apparently faster under more destabilizing conditions. Alternatively, I_{trap} may be destabilized relative to the transition state for folding into I_{open} at moderate GdmCl concentrations.

Is there a consensus refolding pathway for antibody scFv fragments?

These studies on the folding behavior of the scFv fragment 4D5, together with previous reports on such antibody fragments (Freund *et al*. 1996, 1997; 1998; Ramm *et al*., 1999; Jäger & Plückthun, 1997, 1999), highlight the similarities in the folding of this type of protein. The key observation is that independent domain folding is no longer observed in the scFv fragments. Instead of folding rapidly and independently into compact, native-like structures, the domains associate prematurely, before full $^1H/^2H$-exchange protection can be established on the level of the domains. Premature domain association has not been observed in the Fv fragments investigated so far (Jäger & Plückthun, 1999a), suggesting that it is the interdomain peptide linker in the scFv fragment which favors such early non-native domain contacts. Possibly, the linker increases the effective domain concentration early in the reaction coordinate. Premature domain association in the scFv-heterodimers may thus be determined by the ratio of the folding rates of the constituting domains into native-like conformers and the rate of unproductive assembly of the two partially structured domains. As the assembly of two non-native domains might be unspecific and diffusion-controled, the formation of folding traps in the scFv fragments might thus well be the rule rather than the exception. In those systems where the stability of the heterodimer interface is significantly lower than the intrinsic stability of the constituting domains, non-native domain contacts may be reduced by performing refolding studies at sufficiently high denaturant concentrations.

The scFv fragments of different antibodies are believed to be somewhat different in the rates with which they return from the trap, probably a consequence of different stabilities and interface interaction energies. This is reflected in the rate constants other than proline *cis/trans*-isomerization and in which of the open forms are populated to what extent. For example, they may differ in whether they can directly return from the *cis* or *trans*-trapped states. Different solvents may also alter the relative flux through these pathways. The outline mechanism discussed here may be a useful framework to explain these differences. We believe that the further elucidation of the structural features of the on and off-pathway intermediates will be very crucial in the design of further improved molecules with this architecture.

Materials and Methods

Materials

The scFv fragment was expressed from a vector encoding the linked domains in the orientation V_H-$(G_4S)_3$-V_L (Knappik & Plückthun, 1995). A His_5-tag was attached to the C terminus of the V_L domain to facilitate protein purification. For the expression of the isolated V_H domain from the same vector, the gene sequence encoding the peptide linker and the V_L domain was deleted by PCR, and a His_5-tag was attached to the C terminus to facilitate protein purification. The expression vector for the V_L domain was derived analogously.

Protein purification

The domains V_H and V_L and the scFv fragment were separately expressed at 25 °C in the *E. coli* strain JM83 and secreted into the periplasm to allow disulfide bond formation. Cells were grown in LB broth. Protein expression was induced with IPTG at A_{550} and cells were grown for seven hours. Periplasmic extracts were prepared as described (Lindner *et al*., 1992). All chromatographic steps were performed at 4 °C. First, purification to near homogeneity from periplasmic extracts was achieved by immobilized metal ion affinity chromatography (IMAC) (Qiagen), equilibrated in 20 mM sodium borate (pH 7.8), 500 mM NaCl. Bound protein was eluted with a linear imidazole gradient (0-200 mM imidazole in 20 mM Mes (pH 6.0), 500 mM NaCl). The appropriate fractions from IMAC were pooled, dialyzed against 20 mM Mes (pH 6.0) and loaded onto a SP-Sepharose column (Pharmacia), equilibrated in the same buffer. Pure V_L domain was eluted using a linear NaCl-gradient (0-500 mM NaCl in 20 mM Mes (pH 6.0)), dialyzed against 20 mM Mes (pH 6.0) and stored at 4 °C until use. For purification of the V_H domain or the scFv fragment, fractions from IMAC were concentrated, buffer-exchanged against 20 mM Mops (pH 7.0) using a PD10-column (Pharmacia) and loaded onto a Protein-A Sepharose column (Pharmacia), equilibrated in the same buffer. Specifically bound proteins were eluted with 100 mM sodium citrate (pH 3.3). The eluate was immediately neutralized with 1 M Tris (pH 8.0), dialyzed against 20 mM Mes (pH 6.0) and stored at 4 °C. Protein purity was checked by non-reducing SDS-15 % PAGE. Protein concentrations were determined as described by Gill & von Hippel (1989). Protein yields (per liter of culture) were 0.1 mg (V_H domain), 10 mg (V_L domain) and 3 mg (scFv fragment).

Determination of protein stabilities

Steady-state fluorescence experiments were performed at 10 °C with a PTI Alpha Scan spectrofluorimeter (Photon Technologies, Inc., Ontario, Canada). Slit-widths of 2 and 10 nm were used for excitation and emission, respectively. Protein/GdmCl mixtures were prepared from protein solutions (20 mM Mes, pH 6.0) and an 8 M GdmCl stock solution (20 mM Mes, pH 6.0). Exact GdmCl concentrations were determined as described by Pace (1986). After incubation for 24 hours at 10 °C, fluorescence emission spectra were recorded. Excitation was at 280 nm (V_L) or 295 nm (scFv, V_H). For the individual domains, fluorescence emission intensities at a fixed wavelength or the fluorescence emission maximum were plotted *versus* [GdmCl]. The emission maximum was determined by fitting the emission spectrum to a third-order polynomial (Knappik & Plückthun, 1995). Protein stabilities were calculated from these plots by non-linear least-squares fitting to a two-state reaction using a linear free energy model (Santoro & Bolen, 1988) using the program Kaleidagraph (Synergy Software, Reading, USA). For the scFv fragment, which does not follow a two-state behavior, a global fit of the fluorescence intensities between 310 and 420 nm was also carried out, using the program SAVUKA (Bilsel *et al*., 1999; Gualfetti *et al*.,

1999). This package, based on an early version created by Drs D. Lambright and S. Boxer, was developed by Drs O. Bilsel and C. R. Matthews (Pennsylvania State University).

Kinetic experiments

Stopped-flow experiments were performed with an Applied Photophysics model SX-17MV spectrofluorimeter (Leatherhead, England) at 10 °C. Refolding was initiated by a 1:25 (v/v) dilution of unfolded protein (20 mM Mes (pH 6.0), [GdmCl] see the text) into 20 mM Mes (pH 6.0), 200 mM arginine. The reaction was monitored by measuring the change in fluorescence emission at >305 nm or >360 nm. Slit-widths of 1 and 2 mm were used for excitation and emission, respectively. Typically, five to nine fluorescence traces were averaged and fitted to a sum of exponentials using the program Kaleidagraph.

Slow folding reactions were triggered by manual dilution and followed by monitoring the change in fluorescence emission intensity at a fixed wavelength. Two different types of refolding experiments are described in the text. In the first type of experiment, native protein was denatured in 20 mM Mes (pH 6.0), 6 M GdmCl (final concentration) and allowed to equilibrate for at least 12 hours at 10 °C to enable prolyl-peptide bonds to reach *cis/trans*-equilibrium (equilibrium-denatured protein). Refolding was started by a 1:100 dilution of the denatured protein into 20 mM Mes (pH 6.0), 200 mM arginine. In the second type of experiment, native protein was only briefly, but completely, denatured for 20 seconds in 20 mM Mes (pH 6.0), 6 M GdmCl (short-term denatured protein), before the refolding reaction was initiated by a 1:100 dilution into 20 mM Mes (pH 6.0), 200 mM arginine. Fluorescence refolding traces were fitted to a sum of exponentials using the program Kaleidagraph.

^{1}H/^{2}H-exchange experiments

Two types of ^{1}H/^{2}H-exchange experiments are described. In the first type of experiment, refolding was started from an equilibrium-denatured and deuterated protein. To achieve complete deuteration, purified protein was extensively dialyzed against water, lyophilized, dissolved in ^2H_2O-buffer (20 mM Mops (p^{2}H 6.7), containing 6 M GdmCl) and incubated for more than 12 hours at room temperature. The p^{2}H of the solution was not isotope-corrected. For the initiation of refolding, the protein was diluted 1:100 into 20 mM Mops (p^{2}H 6.7), 200 mM arginine, dissolved in ^2H_2O. After various times, the protein was diluted again tenfold into H_2O-buffer containing 50 mM ammonium acetate (pH 6.0) to allow all labile ^{2}H to exchange for ^{1}H. The final volume was typically 10-15 ml. The reaction was then allowed to go to completion (three hours at 10 °C). The protein solution was concentrated at 4 °C (Centricon 10), dialyzed for six hours against 5 mM ammonium acetate (pH 6.0) in ^2H_2O to remove the arginine (buffer was exchanged every two hours), and finally loaded onto a PD-10 column (Pharmacia, Sweden) to remove trace amounts of buffer salts and arginine. The eluate was then concentrated to a final volume of approximately 30-40 µl (Centricon 10) and used directly for mass determination.

A slightly different protocol was used for labeling short-term denatured protein. Native and fully protonated scFv or V_L was first concentrated to ~300 µM. Deuteration was then achieved by a 1:4 dilution of the protein into 20 mM Mops (p^{2}H 6.7), 8 M GdmCl in ^2H_2O. Unfolding of either V_L or the scFv fragment is complete in less than 20 seconds under these conditions (see Results). After 40 seconds incubation in 6 M GdmCl, the protein was further diluted 1:100 into 20 mM Mops (p^{2}H 6.7), 200 mM arginine in ^2H_2O to initiate the refolding reaction. All subsequent steps were performed as described above.

In those experiments where the scFv fragment was refolded from the equilibrium unfolding intermediate (native V_L domain, unfolded V_H domain), the ^{1}H/^{2}H-exchange was performed as follows. First, the scFv fragment was completely unfolded and deuterated as described above (20 mM Mops (p^{2}H 6.7), 6 M GdmCl). Next, the unfolded scFv fragment was diluted 1:3 into 20 mM Mops (p^{2}H 6.7), giving a final GdmCl concentration of 2 M. The solution was then allowed to incubate for 12 hours at 10 °C, which allows the V_L domain to refold into the native state, while the V_H domain remains unfolded. For ^{1}H/^{2}H-exchange, the equilibrium-unfolding intermediate (in 2 M GdmCl) was concentrated to approximately 50 µM (Centricon 10). Refolding reactions from the intermediate were triggered by a 1:20 dilution into 20 mM Mops (p^{2}H 6.7), 200 mM arginine, dissolved in ^2H_2O. After various times, the protein was diluted again tenfold into H_2O-buffer containing 50 mM ammonium acetate (pH 6.0) to allow all labile ^{2}H to exchange for ^{1}H. The final volume was typically 10-15 ml. The reaction was then allowed to go to completion (one hour at 10 °C), and the sample was prepared for mass spectrometry as described above.

Mass spectrometry

Electrospray ionization mass spectra were recorded using an API III triple-quadrupole instrument (PE-Sciex, Ontario, Canada). Protein solutions were infused into the ion source at a flow rate of 8 µl/minute by a syringe pump. The samples were mixed in a 1:1 ratio with precooled methanol containing 0.5 % formic acid, resulting in a pH of approximately 2.5, and 5 µl of this mixture was immediately flow-injected into an ice-cold carrier solution (50 % methanol, 0.25 % formic acid). The use of cooled solutions and the adjustment of the pH value of the protein samples at pH 2.5 for the mass spectrometric measurements were found to minimize ^{1}H/^{2}H-back-exchange significantly (data not shown). An ion spray voltage of 5000 V and an orifice voltage of 75 V were applied for all measurements. The resolution of the mass spectrometer was tuned to give a constant peak width of approximately 1 Da (full half-width maximum) across the mass range of interest. Mass spectra were recorded in the m/z range from 1000 to 2300 Da with a scan step size of 0.2 Da and a scan duration of five seconds.

Acknowledgments

Financial support was from the Schweizerischer Nationalfonds grant B-2006.295.6202. We are indebted to Dr Osman Bilsel (Penn. State University) for his global fit program SAVUKA and his help in using it. We thank Barbara Klinger for help in the purification of the scFv fragment.

References

Bai, Y., Milne, J. S., Mayne, L. & Englander, S. W. (1993). Primary structure effects on peptide group hydrogen exchange. *Proteins: Struct. Funct. Genet.* **17**, 75-86.

Bilsel, O., Zitzewitz, J. A., Bowers, K. E. & Matthews, C. R. (1999). Folding mechanism of the alpha-subunit of tryptophan synthase, an alpha/beta barrel protein: global analysis highlights the interconversion of multiple native, intermediate, and unfolded forms through parallel channels. *Biochemistry,* **38**, 1018-1029.

Brandts, J. F., Hu, C. Q., Lin, L. & Mas, M. T. (1989). A simple model for proteins with interacting domains. Application to scanning calorimetry data. *Biochemistry,* **28**, 8588-8596.

Carter, P., Presta, L., Gorman, C. M., Ridgway, J. B. B., Henner, D., Wong, W. L., Rowland, A. M., Kotts, C. E., Carver, M. E. & Shephard, H. M. (1992a). Humanization of an anti-p185^{HER2} antibody for human cancer therapy. *Proc. Natl Acad. Sci. USA,* **89**, 4285-4289.

Carter, P., Kelley, R. F., Rodrigues, M. L., Snedecor, B., Covarrubias, M., Velligan, M. D., Wong, W. L., Rowland, A. M., Kotts, C. E. & Carver, M. E. (1992b). High level *Escherichia coli* expression and production of a bivalent humanized antibody fragment. *Bio/Technolology,* **10**, 163-167.

Eigenbrot, C., Randal, M., Presta, L., Carter, P. & Kossiakoff, A. A. (1993). X-ray crystal structures of the antigen-binding domains from three variants of humanized anti-p185^{HER2} antibody 4D5 and comparison with molecular modelling. *J. Mol. Biol.* **229**, 969-995.

Freund, C., Honegger, A., Hunziker, P., Holak, T. A. & Plückthun, A. (1996). Folding nuclei of the scFv fragment of an antibody. *Biochemistry,* **35**, 8457-8464.

Freund, C., Gehrig, P., Holak, T. & Plückthun, A. (1997). Comparison of the amide proton exchange behavior of the rapidly formed folding intermediate and the native state of an antibody scFv fragment. *FEBS Letters,* **407**, 42-46.

Freund, C., Gehrig, P., Baici, A., Holak, T. A. & Plückthun, A. (1998). Parallel pathways in the folding of a short-term denatured scFv fragment of an antibody. *Fold. Des.* **3**, 39-49.

Gill, S. C. & von Hippel, P. H. (1989). Calculation of protein extinction coefficients from amino acid sequence data. *Anal. Biochem.* **182**, 319-326.

Goto, Y. & Hamaguchi, K. (1982). Unfolding and refolding of the constant fragment of the immunoglobulin light chain. *J. Mol. Biol.* **156**, 891-910.

Gualfetti, P. J., Bilsel, O. & Matthews, C. R. (1999). The progressive development of structure and stability during the equilibrium folding of the alpha subunit of tryptophan synthase from *Escherichia coli. Protein Sci.* **8**, 1623-1635.

Huyghues-Despointes, B. M. P., Scholtz, M. & Pace, N. C. (1999). Protein conformational stabilities can be determined from hydrogen exchange rates. *Nature Struct. Biol.* **6**, 910-912.

Jaenicke, R. (1987). Folding and association of proteins. *Prog. Biophys. Mol. Biol.* **49**, 117-237.

Jäger, M. & Plückthun, A. (1997). The rate-limiting steps for the refolding of an antibody scFv fragment. *FEBS Letters,* **418**, 106-110.

Jäger, M. & Plückthun, A. (1999a). Folding and assembly of an antibody Fv fragment, a heterodimer stabilized by antigen. *J. Mol. Biol.* **285**, 2005-2019.

Jäger, M. & Plückthun, A. (1999b). Domain interactions in antibody Fv and scFv fragments: effects on unfolding kinetics and equilibria. *FEBS Letters,* **462**, 307-312.

Kabat, E. A., Wu, T. T., Perry, H. M., Gottesman, K. S. & Foeler, C. (1991). NIH Publication no. 91-3242, National Institute of Health, Bethesda, MD.

Kelley, R. F., O'Connell, M. P., Carter, P., Presta, L., Eigenbrot, C., Covarrubias, M., Snedecor, B., Bourell, J. H. & Vetterlein, D. (1992). Antigen binding thermodynamics and antiproliferative effects of chimeric and humanized anti-p185^{HER2} antibody F_{ab} fragment. *Biochemistry,* **31**, 5434-5441.

Knappik, A. & Plückthun, A. (1995). Engineering turns of a recombinant antibody improve its *in vivo* folding. *Protein Eng.* **8**, 81-89.

Lilie, H. (1997). Folding of the F_{ab} fragment within the intact antibody. *FEBS Letters,* **417**, 239-242.

Lilie, H., Rudolph, R. & Buchner, J. (1995). Association of antibody chains at different stages of folding: Prolyl isomerization occurs after formation of quaternary structure. *J. Mol. Biol.* **248**, 190-201.

Lindner, P., Guth, B., Wülfing, C., Krebber, C., Steipe, B., Müller, F. & Plückthun, A. (1992). Purification of native proteins from the cytoplasm and periplasm of *Escherichia coli* using IMAC and histidine tails: a comparison of proteins and protocols. *Methods: Comput. Methods Enzymol.* **4**, 41-56.

Myers, J. K., Pace, C. N. & Scholtz, J. M. (1995). Denaturant m values and heat capacity changes: Relation to changes in accessible surface areas of protein unfolding. *Protein Sci.* **4**, 2138-2148.

Pace, C. N. (1986). Determination and analysis of urea and guanidine hydrochloride denaturation curves. *Methods Enzymol.* **131**, 266-280.

Padlan, E. A. (1994). X-ray crystallography of antibodies. *Advan. Protein Chem.* **49**, 57-133.

Ramm, K., Gehrig, P. & Plückthun, A. (1999). Removal of the conserved disulfide bridges from the scFv fragment of an antibody: effects on folding kinetics and aggregation. *J. Mol. Biol.* **290**, 535-546.

Ramsay, G. & Freire, E. (1990). Linked thermal and solute perturbation analysis of cooperative domain interactions in proteins. Structural stability of diphtheria toxin. *Biochemistry,* **29**, 8677-8683.

Santoro, M. M. & Bolen, D. W. (1988). Unfolding free energy changes determined by the linear extrapolation method. 1. Unfolding of phenylmethanesulfonyl chymotrypsin using different denaturants. *Biochemistry,* **27**, 8063-8068.

Satow, Y., Cohen, G. H., Padlan, E. A. & Davies, D. R. (1986). Phosphorylcholine binding immunoglobulin F_{ab} McPC603. *J. Mol. Biol.* **190**, 593-604.

Schmid, F. X. (1986). Fast-folding and slow-folding forms of unfolded proteins. *Methods Enzymol.* **131**, 70-82.

Steipe, B., Schiller, B., Plückthun, A. & Steinbacher, S. (1994). Sequence statistics reliably predict stabilizing mutations in a protein domain. *J. Mol. Biol.* **240**, 188-192.

Tsunenaga, M., Goto, Y., Kawata, Y. & Hamaguchi, K. (1987). Unfolding and refolding of an immunoglobulin light chain and its variable and constant fragments. *Biochemistry,* **26**, 6044-6051.

Wörn, A. & Plückthun, A. (1998a). A stable scFv fragment can tolerate the loss of both disulfide bonds and fold correctly. *FEBS Letters*, **427**, 357-361.

Wörn, A. & Plückthun, A. (1998b). Mutual stabilization of V_L and V_H in single-chain antibody fragments, investigated with mutants engineered for stability. *Biochemistry*, **37**, 13120-13127.

Wörn, A. & Plückthun, A. (1999). Different equilibrium stability behavior of scFv fragments: indentification, classification and improvement by protein engineering. *Biochemistry*, **38**, 13120-13127.

Wörn, A. & Plückthun, A. (2001). Stabilization of antibody scFv fragments. *J. Mol. Biol.* in the press.

Edited by C. R. Matthews

(Received 4 October 2000; accepted 13 November 2000)